LA-UR 93-1393

TITLE: TWO-DIMENSIONAL SIMULATIONS OF FOIL IMPLOSION EXPERIMENTS ON THE LOS ALAMOS CAPACITOR BANK

AUTHOR(S): D. L. Peterson
R. L. Bowers
J. H. Brownell
A. E. Greene
H. Lee
W. Matuska

SUBMITTED TO: Third International Conference on Dense Z-Pinches
19-23 April 1993
Imperial College, London

DISCLAIMER

MASTER

Los Alamos National Laboratory
Los Alamos, New Mexico 87545

DISTRIBUTION OF THIS DOCUMENT IS UNLIMITED

TWO-DIMENSIONAL SIMULATIONS OF FOIL IMPLOSION EXPERIMENTS ON THE LOS ALAMOS PEGASUS CAPACITOR BANK

D. L. Peterson, R. L. Bowers, J. H. Brownell,
A. E. Greene, H. Lee, and W. Matuska
Los Alamos National Laboratory, Los Alamos, NM 87544

ABSTRACT

A number of z-pinch experiments have been conducted at Los Alamos on the Pegasus capacitor bank in which 2-cm high, 5-cm radius, thin foil loads were imploded with currents in excess of 3 MA. Two-dimensional radiation magnetohydrodynamic (RMHD) simulations of these implosions have been performed to model the implosion dynamics and subsequent generation of an x-ray pulse. Comparison of the simulation instability development with visible light framing camera photographs show good agreement and illustrate the instability evolution from short to long wavelengths and a final disruption of the imploding plasma shell. The calculations also show good agreement with experimental timing and measured current and voltage waveforms, and also reproduce features characteristic of the x-ray output. These include a broad pulsewidth, and the presence of multiple peaks and small time scale structures, features which cannot be reproduced by one-dimensional models. X-ray spectra obtained from the calculated pinch also reproduce qualitative features in the measured spectra.

INTRODUCTION

The magnetic implosion of cylindrical, conducting loads has been used in pulsed power experiments for decades as a source of soft x-rays.[1] The Los Alamos Foil Implosion program is developing imploding plasmas as an x-ray source, with the ultimate goal being a 1 to 10 MJ radiation source, delivered in a pulse of greater than 100 TW power. The prime power source could be a large capacitor bank or an explosive flux compression generator.[2] Experiments have been designed and fielded with thin (several thousand angstrom thick) cylindrical aluminum foil loads, typically 5 cm in radius and 2 cm high. In this paper we discuss computational modeling and the results of experiments in which 4.9 mg and 13.0 mg aluminum loads were imploded on the Pegasus capacitor bank facility. In these experiments the bank delivered about 4 MA to the load over a period of about 2 μs.

One dimensional (1 D) models of these implosions generally predict efficient conversion of magnetic energy into x ray output and radiation pulsewidths that are very short (full width at half maximum under 5 ns). The imploding plasma is, however, subject to the development of magnetically driven Rayleigh Taylor instabilities. As a result of this instability growth, the radiation pulse is broadened and the maximum power is reduced. Understanding the development of the instabilities and how they effect the radiation pulse, as well as being able to properly simulate experiments which show the effects of the instabilities, is the first step in designing implosion loads which will produce higher quality radiation pulses.

We have studied the physics of the imploding plasmas using two codes: a 1-D RMHD Lagrangian code, which can simulate the development of the solid foil through melt, vaporization, and the formation of the plasma; and a 2-D RMHD Eulerian code which is well suited to examining instability growth. Both codes use SESAME equation-of-state tables and are self-consistently coupled to ladder circuit networks, which simulate the capacitor bank and associated power-flow hardware. The 2-D simulations begin with profiles of density, temperature, velocity, and magnetic field provided from the 1-D simulation at a point after the plasma has expanded from the original thin solid foil (typically, the point of maximum expansion of the plasma is used). Perturbations in the density of the plasma are then imposed to mock-up variations which arise in the experiment. These perturbations then seed the growth of magnetically driven Rayleigh-Taylor instabilities. The simulations can then be compared with experiments where the effects of the instability development are seen not only in the observed radiation pulse, but in current and voltage waveforms, in visible light framing camera photos of the imploding plasma, in time-integrated x-ray pinhole photos of the stagnation region, and in time-dependent spectroscopy measurements.

2-D INSTABILITY DEVELOPMENT

In a typical 2-D simulation, the instability development is seeded by the imposition of random density variations on the 1-D density profile in a range between $-\delta$ and $+\delta$ (typical values of δ are between 5% and 20%). Random perturbations allow the development of a range of instability wavelengths, with shorter wavelengths growing fastest. In general, the results are insensitive to the exact pattern of the initial random perturbations.

Figure 1 shows the instability growth in a simulation using a 20% random density perturbation. Shown in Fig. 2 are the current and radiation pulse profiles for a 1-D simulation and for the 2-D perturbed simulation. The peaks of the two radiation pulses in Fig. 2 have been normalized to a value of 2.0 in each case for ease of comparison (the 2-D peak is much lower than the 1-D peak, representing a lower peak temperature). Figure 2 also shows structure in the 2-D radiation pulse and current waveforms which is absent in 1-D.

As may be seen in the density contours in Fig. 1a, the initial short wavelength modes saturate and give way to longer wavelengths, with a dramatic "bursting" of a Rayleigh-Taylor bubble through the plasma shell shown at the last time. From the viewpoint of the external circuit drive, the inductance change in the implosion remains essentially like that in 1-D until about 1.5 μs (third time shown in Fig. 1b). Note that the linear instability growth regime occurs during the initial part of this time, and thus it is the nonlinear development that is paramount in the

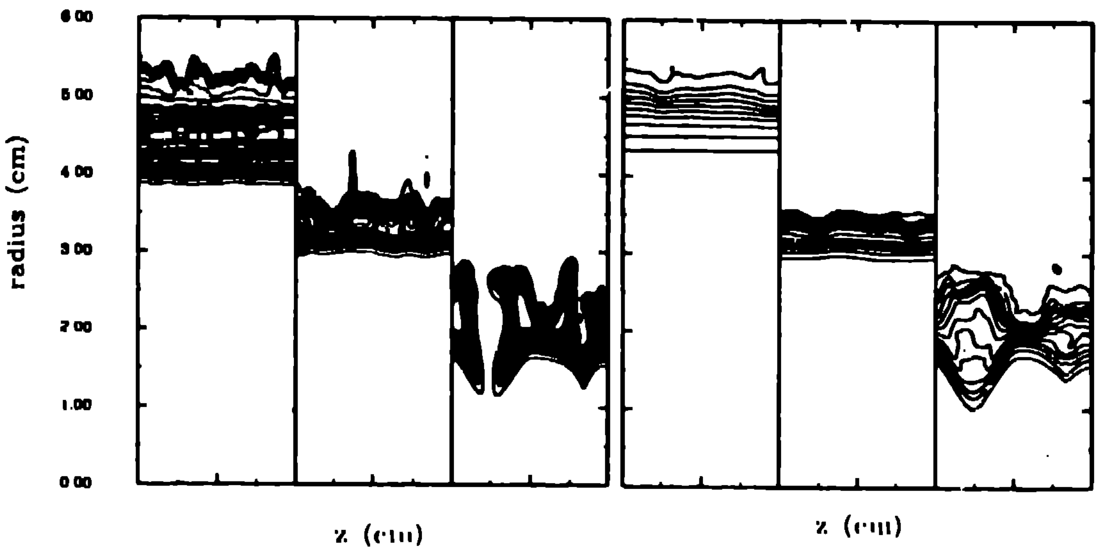

Fig. 1. (a) 2-D simulation isodensity contours in the $r - z$ plane for a perturbed implosion of a 4.9 mg load at times t = 1.1, 1.5 and 1.7 μs. (b) Current streamlines (contours of rB_θ) at the same times as shown in (a).

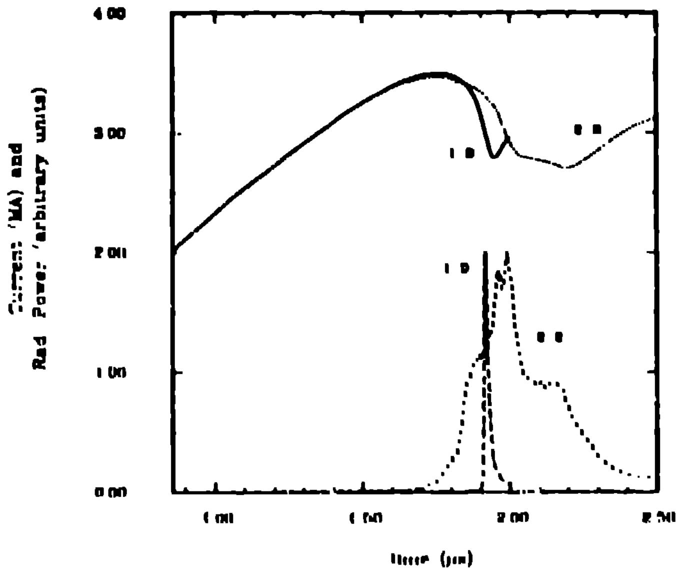

Fig. 2. Currents (solid and dotted curves, in MA) and radiation power (dot dash and dash curves, arbitrary units, scaled to a peak value of 2.0) for 1 D and 2 D simulations of a 4.9 mg load.

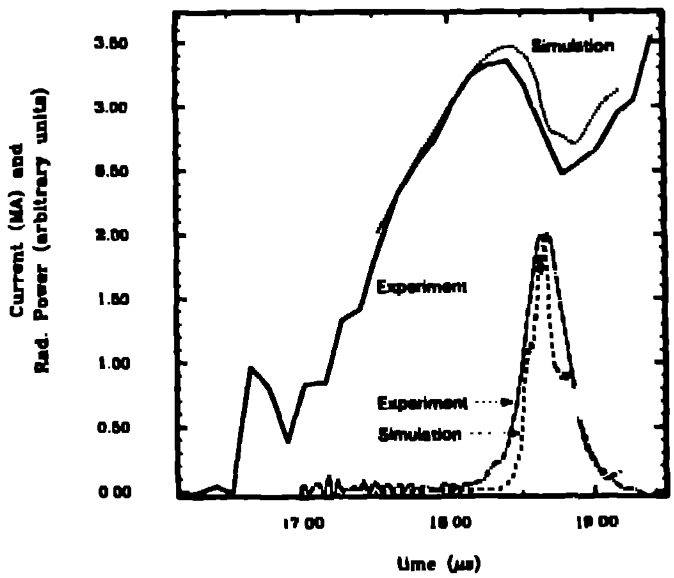

Fig. 3. Experimental current (solid) and x-ray diode (XRD) radiation measurement (dot-dash) compared with a 2-D simulation current (dot) and radiation power (dash) for the 4.9 mg implosion experiment. Current is shown in MA, and the XRD signal and radiation power have both been scaled to a peak value of 2.0 in arbitrary units.

dynamics of the imploding shell. Significant effects begin to arise at the point of bubble burst when magnetic field and a small amount of material are driven to the axis. The change of inductance in this process causes the current to drop, or rise at a reduced rate, and at the same time the radiation pulse begins (as seen at 1.7 μs in Fig. 2). The current path then changes to allow flow between the instability spikes, which effectively saturates further development of the instability. When sufficient material drifts into the region between the spikes to support current flow, a re-acceleration occurs of the main plasma shell, resulting in a final pinch and radiation pulse, and a local current minimum. This may be seen at 2.2 μs in Fig. 1. The relative timing, radiation pulse shape and width, and current waveform thus reveal information about the instability growth

EXPERIMENT WITH A 2500 Å Al FOIL

The first experiment to be discussed here was conducted with a 5 cm radius, 2 cm high, 2500 Å thick aluminum foil with a 1000 Å backing of parylene (for a total mass of 4.9 mg). Simulation comparisons with this experiment (Fig. 3) show good agreement in timing and peak current and in the radiation pulsewidth. Note in particular the beginning of the x ray pulse coincides with the point at which the current begins to turn over, in agreement with the mechanism of the bubble burst through the plasma shell described earlier.

Figure 4 shows a comparison between the computational model and the optical framing camera data at several times during the implosion. The comparison

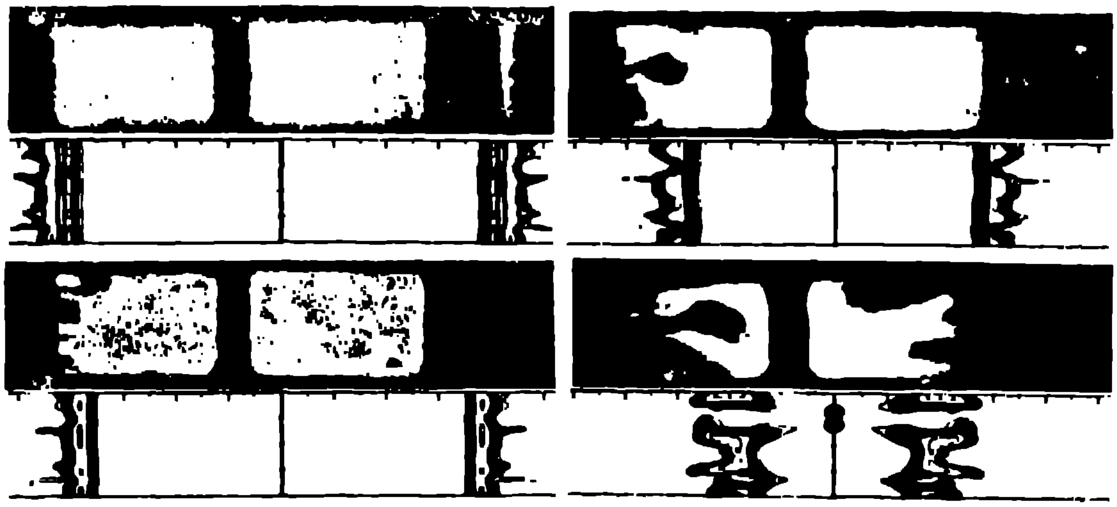

Fig. 4. Visible light framing camera pictures (above) paired with density contours from the corresponding 2-D simulation (below) at four times during the 4.9 mg implosion (earliest time at upper left, last time at lower right). The pictures and plots are to scale and viewed side-on. Three return conductors block part of the view in the photos (at extreme left, near the center, and at the right).

shows the development of short to long wavelength modes in both the experiment and the simulation with good agreement in the instability wavelength and amplitude. In the last frame shown, bubble burst has occurred, coincident with the start of radiation and the turn over in the current. Also at this time, a tilt in the pinch can be perceived, exhibiting 3-D effects. We find excellent agreement between amplitude and lengthscale of the features in the instability growth prior to the onset of 3-D effects.

The data from the 4.9 mg implosion demonstrates that magnetic instabilities are present, that the x-ray pulsewidth is broader than predicted by 1-D models, and that a simple randomly perturbed initial model can reproduce many of the observed features of the implosion. In this model the adjustable parameter is the amplitude of the density perturbations, and the best fit to the data is obtained with an amplitude of $\delta = 20\%$.

EXPERIMENTS WITH 7500 Å Al FOILS

Based upon the experience of the first experiment, simulations were performed for foils of increased mass. These simulations indicated that for a similar initial perturbation level, there should be substantially less instability development and a narrowing of the radiation pulse. Two experiments using an Al thickness of 7500 Å with a backing of 1000 Å of parylene (for a total mass of 13.0 mg) are discussed in this section

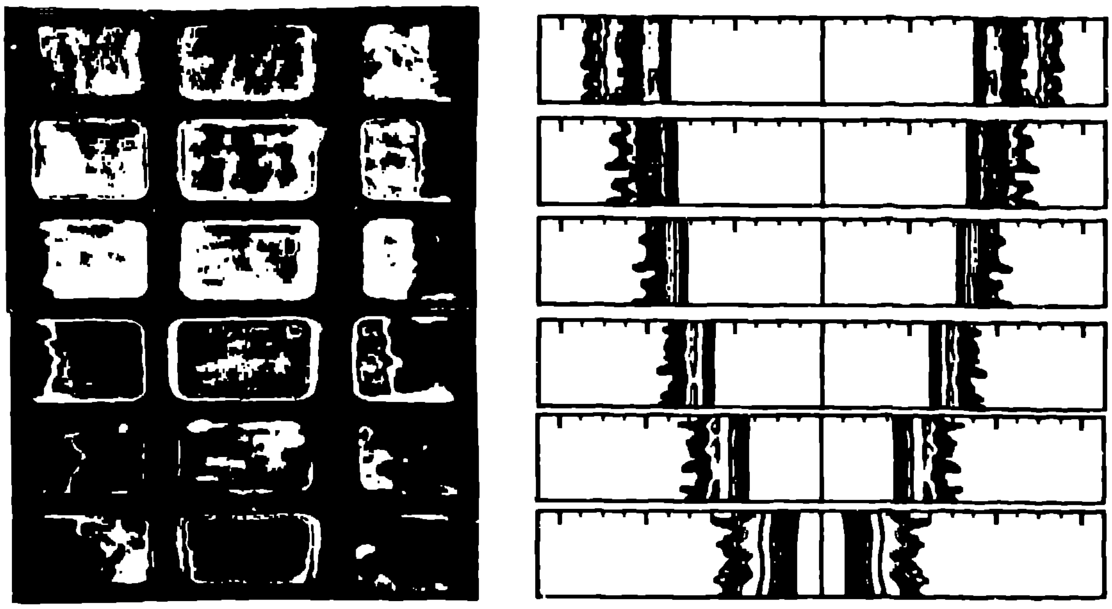

Fig. 5. Visible light framing camera pictures (left) paired with density contours from the corresponding 2-D simulation (right) for the first 13.0 mg implosion. The pictures and plots are to scale and viewed side on. Three return current conductors block part of the view in the photos (at extreme left, center left, and center right).

The first of these experiments suffered a short (probably caused by a vacuum leak, which may also have introduced additional material into the system) in the power flow system. This resulted in a reduced current delivered to the load, especially at late time when the instability growth is most dramatic. The 2-D simulation of the experiment therefore imposed the measured current to drive the load, rather than using the self consistent circuit model, since the nature of the short is unknown. The instability development, as captured by the framing camera photography, provided an excellent comparison with that of the simulation as can be seen in Fig. 5. The photos show clear evidence of banding, which may be interpreted as variations associated with 2-D axisymmetric instabilities. Again, the evolution from short to long wavelength growth can be seen, as well as good correlation between the observed and calculated instability amplitudes. We do not expect the exact distribution in the r – z plane to be the same in the experiment and simulation as this distribution would depend on the exact random density pattern imposed initially. This implosion seemed to have better stability properties, though the reason for this may have been due to the reduction of the drive current.

The second experiment, also using a 7500 Å Al foil, failed to produce framing camera data, but was otherwise successfully diagnosed. The radiation pulsewidth was not reduced, but rather increased, suggesting a higher level of initial perturba-

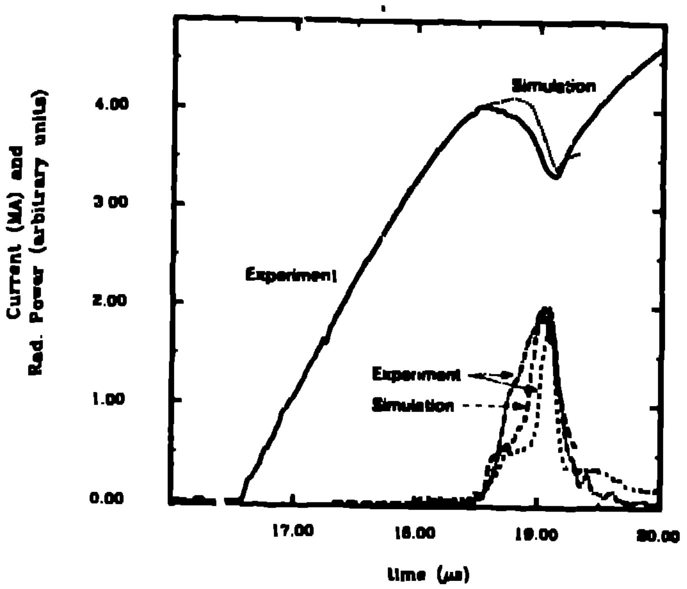

Fig. 6. Experimental current (solid) and two XRD radiation measurements (dot-dash and short-dash, representing two energy filterings) compared with a 2-D simulation current (dot) and radiation power (long-dash) for the the second 13.0 mg implosion experiment. Current is shown in MA, and the XRD signals and radiation power have been scaled to a peak value of 2.0 in arbitrary units.

tion than had been seen previously. In this case, the experiment was best matched computationally by assuming an initial perturbation consisting of four "notches" imposed early in the implosion. These may correspond to wrinkles which were observed in the foil. Comparison between this simulation and measured current and two XRD traces (representing differing filters) is shown in Fig. 6. Timing, peak current, and features in the radiation pulse are all in very good agreement. Comparisons of $\frac{dI}{dt}$ and the inferred voltage at the load (Fig. 7) also show agreement with the features of bubble burst and re-acceleration of the shell evident in their structure. Time integrated x-ray pinhole photos also indicate two bright regions near each electrode, consistent with an examination of time-integrated radiation energy on-axis in the simulation.

Another diagnostic, the time dependent x-ray spectrometer, is currently undergoing a period of development as applied to Pegasus experiments. Side-on spectra from the cylindrically symmetric 2-D simulation were calculated using ray tracing and SESAME multi-group opacities. This comparison showed an encouraging correlation of major features (main peak, valley and high $h\nu$ peak) in the experimental spectrum which also appear in the calculation. A more detailed discussion of this comparison is given in a companion paper.[3]

CONCLUSIONS

Comparisons between the experimental results of Pegasus implosion data with 2-D simulations reveal good agreement in timing (especially relative timing

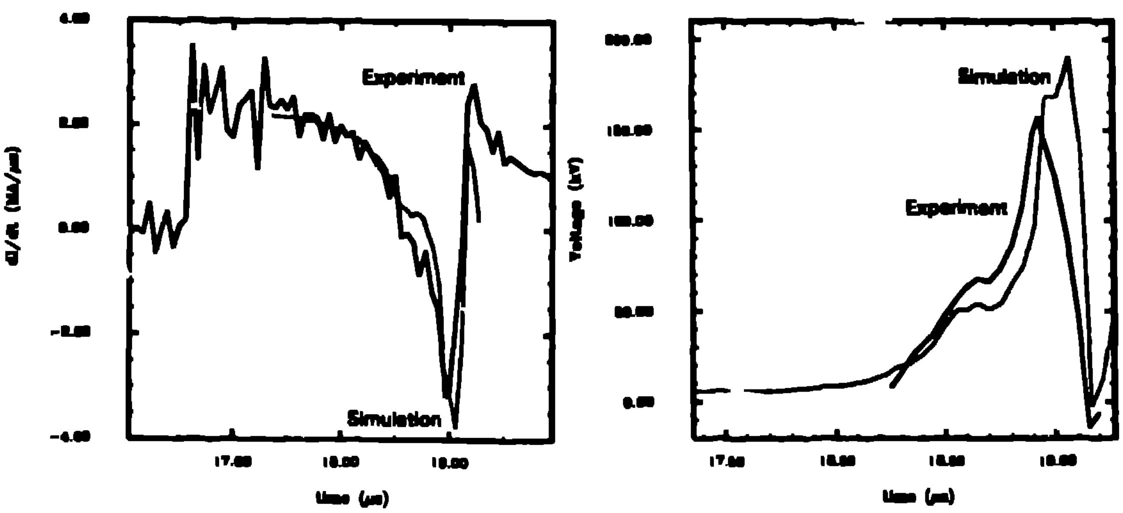

Fig. 7. Experimental (solid) and 2-D simulation (dot) curves of $\frac{dI}{dt}$ (left) and voltage (right) for the second 13.0 mg implosion experiment.

between features in the drive current and the radiation pulse), waveform shape, and radiation pulsewidth. There is substantial difference between 2-D and 1-D results, due to the development of the Rayleigh-Taylor instabilities which show a pattern of growth from short to long wavelength, a "bursting" of the bubble regions through the plasma shell, and finally electrical shorting across the spike regions allowing a re-acceleration of the plasma shell. These features are evidenced in the current and radiation pulse shapes. In addition, framing camera pictures have verified the presence of instabilities as indicated in the 2-D simulations. Time-dependent spectroscopy measurements have also been compared with the simulation with encouraging results. The experiments have thus provided an important benchmark in verifying our capability to simulate the implosion physics, and the understanding provided by the simulations has helped to explain the complex development seen in these experiments.

REFERENCES

1. P. J. Turchi and W. L. Baker, J. Appl. Phys. 44, 4963, (1973).
2. J. Brownell *et al.*, Proceedings of the 9th International Conference on High Power Particle Beams (1992, to be published).
3. W. Matuska *et al.*, these proceedings.